Coordination Chemistry Reviews, 120 (1992) 281–307
Elsevier Science Publishers B.V., Amsterdam

Paramagnetism and dynamic properties of electrons and nuclei

Claudio Luchinat[1]* and Zhicheng Xia[2]
[1] *Institute of Agricultural Chemistry, University of Bologna, Bologna (Italy)*
[2] *Relaxometry Centre, Department of Chemistry, University of Florence, Florence (Italy)*

(Received 21 October 1991)

CONTENTS

A. INTRODUCTION

One of the very first of the many contributions by Luigi Sacconi to the advancement of science was on the, at that time, mysterious hydrated molybdenum blue [1], a paramagnetic compound. Sacconi, together with Cini, soon developed an accurate instrumental setup for measuring magnetic susceptibilities [2], and pioneered the discovery and characterization of novel, and sometimes unexpected, paramagnetic coordination compounds [2–5].

Paramagnetism is a well-known property of matter. Unlike ferromagnetism, however, it does not impart macroscopic properties to matter which are of obvious relevance in everyday life. Yet, as Sacconi soon pointed out, paramagnetism is a central feature of many chemical substances, particularly many coordination compounds, and its understanding in all of its manifestations is of special importance because paramagnetism is closely related to fundamental properties of the particles constituting matter. Understanding paramagnetism bears implications in the understanding of chemical bonds, electronic energy levels, electron distribution in mole-

* To whom correspondence should be addressed.

cules, and chemical dynamics on very small time scales. In turn, this understanding has impact in applications ranging from biochemistry to material science, pharmacology, medicine, etc.

Since early times, the Sacconi school developed studies of paramagnetic compounds through magnetic and spectroscopic measurements (see the review by Gatteschi in this volume). These studies aimed at obtaining a *static* description of the compounds (stereochemistry and electronic structure). On the other hand, paramagnetism is, if possible, even richer in *dynamic* information. It is the opinion of the senior author, who is proud of being the youngest of Sacconi's offspring, that an ideal continuation of Sacconi's school could be in the direction of understanding the time-dependent phenomena associated with paramagnetism.

In this review, we will deal specifically with the coupling of the unpaired electron spin with magnetic nuclei. This theme has been developed by the senior author in the past 15 years, first under the guidance of, and then together with Ivano Bertini. We will show that the effects of the electron nucleus coupling on the nuclear properties yield direct and sometimes not otherwise obtainable information on electron relaxation and, in particular, on the dynamic aspects of the phenomenon. In turn, electron relaxation is intimately linked to chemical dynamics at a level that goes beyond the molecular scale.

B. THE CONCEPT OF RELAXATION

Any ensemble of particles, characterized by a ladder of quantized energy states, undergoes the phenomenon of relaxation. Boltzmann's Law states that, at any given time, the fraction of particles being in the energy state E_i is given by

$$f_i = \frac{\exp(-E_i/kT)}{\Sigma_i \exp(-E_i/kT)} \tag{1}$$

Although the distribution is constant with time, the single particles may change state by adsorbing or liberating energy under some appropriate form. That the particles can adsorb and liberate energy is demonstrated by spectroscopy. If energy is given to the system, the energy distribution is altered but, after the perturbation, the system spontaneously returns to Boltzmann equilibrium.

We are interested here in the energy level splitting originated in the system by the presence of an external magnetic field, and in the spontaneous transitions among these levels. The transition energies for the most common magnetic fields are typically in the microwave region for electron spin states (EPR spectroscopy) and in the radio wave region for nuclear spin states (NMR spectroscopy). Unlike other spectroscopies, the spontaneous transitions between an excited state and the ground state of an electron spin or a nuclear spin are very unlikely to occur by direct emission of a photon of that energy. Rather, transitions are induced by coupling of the spin system with fluctuating magnetic fields randomly generated in the environment (called the

"lattice" by extension of the term used for crystalline solids) by motions of particles, electric changes, other magnetic dipoles, and so on. Understanding electron and nuclear relaxation mechanisms can therefore lead to the understanding of the dynamic processes occurring in the lattice, in time scale ranges, typically of the order of, or shorter than, the electron or nuclear relaxation times, respectively. This is separately true for both electron relaxation and nuclear relaxation. Furthermore, in paramagnetic systems, nuclear relaxation can give direct information on electron relaxation itself, every time the main mechanism of nuclear relaxation is coupling with the fluctuating magnetic field produced by the electron magnetic moment [6].

C. ELECTRON–NUCLEUS COUPLING AND NMRD

When a paramagnetic compound is dissolved in a solvent, the relaxation rates of solvent nuclei are dramatically enhanced. The enhancement is a linear function of the concentration of added compound. For a fixed concentration, the enhancement depends on (a) the nature of the metal ion, (b) the magnetic field, (c) the availability of coordination sites for solvent molecules, (d) the temperature, (e) the size of the paramagnetic molecule, and (f) the presence of solutes that increase the viscosity of the solution. How we arrive at an understanding of all these effects on a quantitative basis is the subject of this review. For simplicity, but without loss of generality, we will mainly restrict ourselves to the analysis of the water proton longitudinal relaxation rates in the presence of paramagnetic metal aqua ions as solutes.

As anticipated, spin relaxation arises from random fluctuations, in time, of the coupling energy between the spin magnetic dipole and a magnetic field, or magnetic dipole, in the lattice. In the case of a nuclear spin in a paramagnetic substance, the largest source of relaxation is often the coupling to the electron spin magnetic dipole [6–10]. The dipole–dipole interaction Hamiltonian is

$$\mathcal{H} = -g_e \mu_B g_N \mu_N \left[\frac{\hat{I} \cdot \hat{S}}{r^3} - \frac{3(\hat{I} \cdot \hat{r})(\hat{S} \cdot \hat{r})}{r^5} \right] \tag{2}$$

where g_e and g_N are the electron and nuclear g factors, μ_B and μ_N the electron and nuclear Bohr magnetons, $\hat{I}$ represents the nuclear spin, $\hat{S}$ the electron spin, and r the electron–nucleus distance. In some cases, among which is the interaction of water protons with paramagnetic metal ions, r can be successfully approximated by the metal–proton distance [11,12] although, in principle, the electron is not completely localized at the metal nucleus.

This feature allows us to avoid considering the effects of fractional unpaired electron density on the oxygen atom, and to postpone the treatment of that part of the dipolar coupling arising from the limiting case $r = 0$, and known under the name of contact or scalar coupling [8,9]. Contact coupling can be included in the treatment of nuclear relaxation phenomena, whenever needed, by arguments analogous to those

developed hereafter. A new example where contact coupling is relevant will be given later.

Fluctuations in the eigenvalues of Hamiltonian (2) can arise by changes in (a) the $\hat{r}$ modulus, (b) the $\hat{r}$ orientation, and (c) the sense of $\hat{S}$. Physically, these correspond to (a) changes in the metal–nucleus distance, i.e. detachment of the coordinated water molecule, (b) rotation of the metal–aqua complex with respect to the external magnetic field, and (c) electron spin relaxation. Each of the above processes is a random process and, therefore, leads to nuclear relaxation.

The equation for the nuclear longitudinal relaxation rate enhancement caused by dipolar coupling to an electron spin $\hat{S}$ (Solomon's equation) is [7]:

$$T_{1M}^{-1} = \frac{2}{15}\left(\frac{\mu_0}{4\pi}\right)^2 \frac{\gamma_N^2 g_e^2 \mu_B^2 S(S+1)}{r^6}\left[\frac{\tau_c}{1+(\omega_I-\omega_S)^2\tau_c^2} + \frac{6\tau_c}{1+(\omega_I+\omega_S)^2\tau_c^2} + \frac{3\tau_c}{1+\omega_I^2\tau_c^2}\right] \tag{3}$$

where ω_I and ω_S are the nuclear and electronic Larmor precession frequencies, τ_c is the correlation time, γ_N is the magnetogyric ratio, S is the total electron spin, and r is the distance between the nucleus and the paramagnetic ion.

It should be immediately stressed that eqn. (3) holds [7] only for the ideal case of the $\hat{S}$ spin being described by the spin Hamiltonian

$$\hat{\mathcal{H}} = g_e \mu_B B_0 \cdot \hat{S} \tag{4}$$

i.e. in the absence of g-anisotropy, hyperfine coupling with nuclei other than the one observed in the NMR experiment, zero field splitting of the S manifold for $S > 1/2$, and the existence of more than one electron relaxation time (for $S > 1$ in the presence of zero field splitting). Even though real systems can seldom be described or even approximated by Hamiltonian (4) [13], eqn. (3) is often used beyond its validity limits. This still happens today, when different treatments are available to treat properly many of the cases of real interest for which eqn. (3) breaks down (see Sect. H). It is nevertheless useful to examine cases where eqn. (3) holds to start appreciating the information content of nuclear magnetic relaxation measurements. This will be done after describing the instrumental setup to perform these measurements in an appropriate way (Sect. D).

The functional form of eqn. (3) immediately suggests that a satisfactory analysis of relaxation data in terms of the parameters contained in it (minimally r and τ_c) requires the collection of good nuclear relaxation rate values over a wide range of magnetic field. The theoretical field dependence of T_{1M}^{-1} according to eqn. (3) is shown in Fig. 1. Note that the magnetic field scale is logarithmic and that the full coverage of a "dispersion" region, i.e. the region where T_{1M}^{-1} is field-dependent, requires taking data over about two orders of magnitude of magnetic field values. The two dispersions are separated by about three orders of magnitude ($\omega_S/\omega_I = 658$ for I being a proton spin, or more for other nuclear spins) so that a full coverage would require about

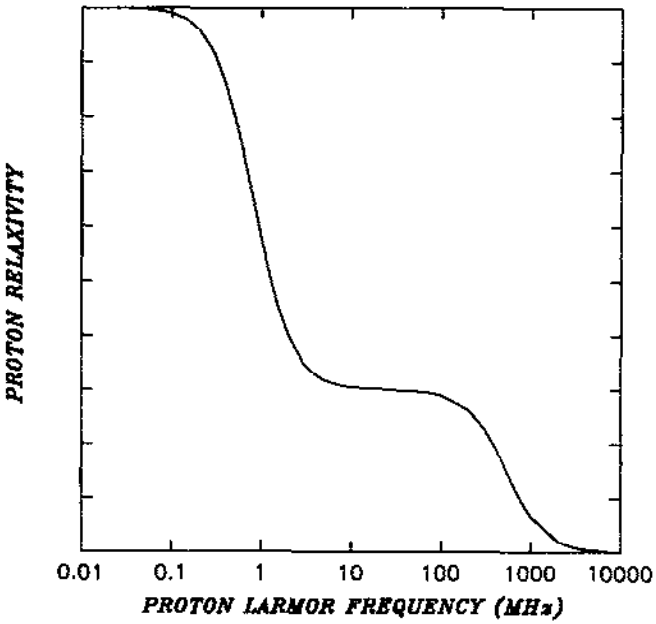

Fig. 1. Theoretical field dependence of T_{1M}^{-1} according to the Solomon equation (eqn. (3)). The curve has been calculated using $\tau_c = 3 \times 10^{-10}$ s. The T_{1M}^{-1} (expressed as relaxivity, see Sect. E) is reported on an arbitrary scale.

five orders of magnitude of magnetic field. As will be apparent in the following, the ω_s dispersion may occur at quite low field so that it is essential that the available magnetic field range be extended to the low-end side more than to the high-end side. A set of nuclear relaxation measurements as a function of magnetic field constitutes what we will call a nuclear magnetic relaxation dispersion (NMRD) profile [14]. The present upper limit for commercial NMR instruments is 600 MHz ^{1}H resonance frequency, corresponding to $\omega_I = 3.77 \times 10^9$ rad s^{-1} and $\omega_s = 2.48 \times 10^{12}$ rad s^{-1}. At the low end, there are desk-top NMR instruments working at 20 MHz ($\omega_I = 1.26 \times 10^8$ rad s^{-1}, $\omega_s = 8.27 \times 10^{10}$ rad s^{-1}). The latter values are still too high to cover many cases of low frequency dispersions. Non-commercial instruments are available which dramatically extend the magnetic field range downwards by more than three orders of magnitude. Here, we describe in detail one of these instruments, the field-cycling relaxometer.

D. FIELD CYCLING RELAXOMETRY

The origin of the field cycling (FC) technique goes back to the early fifties when several research groups, for different reasons, became interested in low-field NMR measurements [15–23]. However, it took more than 20 years to develop this technique [24–33]. After 1975, various prototypes of powerful machines were described

in the literature by groups from Belgium, France, Germany, Great Britain, U.S.A. and Yugoslavia [34–39], and an increasing number of researchers now try to make use of the FC method.

A typical FC sequence involves, generally, three phases in a cycle [40] (Fig. 2), namely the polarization or magnetization period, P, the evolution or relaxation period, E, and the detection or measurement period, D. The sequence in the present version of the Koenig–Brown relaxometer [14,21,23,34,41,42] is as follows [6,14,43]. The cycles start with P, where we have a field B_{0P} as high as possible (50 MHz at present) with moderate requirements on homogeneity. Then, during E, the field is made adjustable in the range $0 < B_{0E} < B_{0P}$. Finally, before D, the intensity of the magnetization is increased again as far as practical ($B_{0D} = 7.5$ MHz at present), but now with sufficient homogeneity to allow NMR signal detection; a 90–180° pulse sequence is applied and the amplitude of the subsequent echo, which is proportional to the magnetization at the end of relaxation period, is measured.

In order to enhance the change of magnetization during the relaxation period, and hence to improve the sensitivity of field cycling, two FC sequences are used

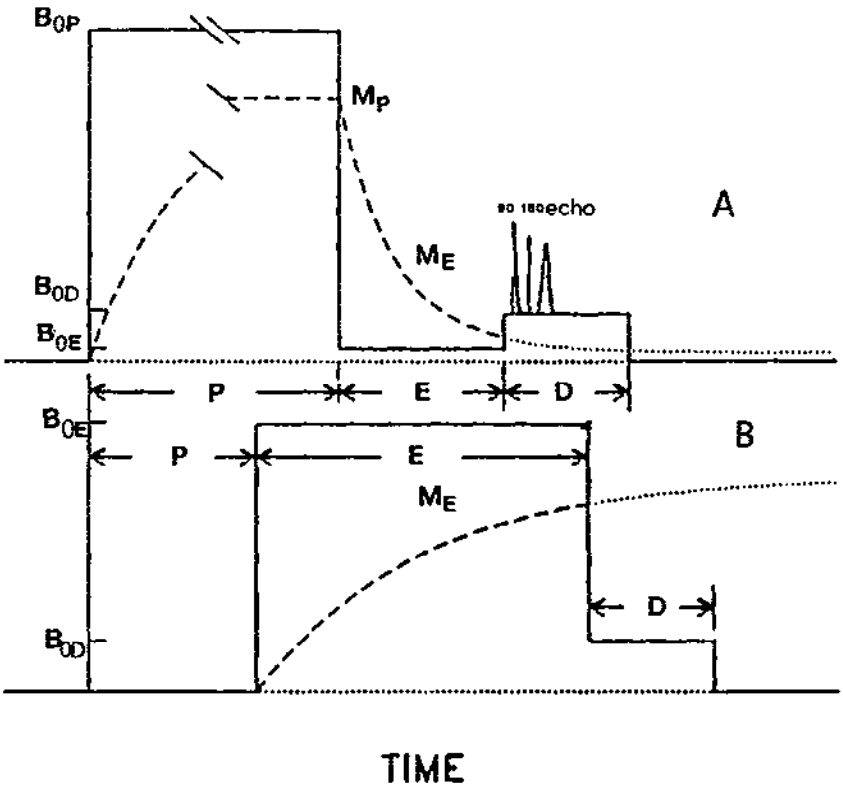

Fig. 2. Field cycling sequences in the "pulse down" (A) and "pulse up" (B) modes of the Koenig–Brown relaxometer (see text). Full lines indicate magnetic field, broken lines indicate sample magnetization.

according to whether the magnetic field (B_{0E}), at which we perform the relaxation measurement, is relatively high or relatively low. Relaxation rates at the lower values of B_{0E} are more difficult to measure by other techniques, and it is for this range that an FC relaxometer makes possible good sensitivity with relatively small samples; we describe this case first. The FC sequence used, called "pulse-down", is as follows (Fig. 2A). The field is brought to B_{0E} from a field B_{0P}, or "soak field", which has been applied for a time P, a time long enough for the magnetization of the proton spin to have reached its equilibrium magnetization at B_{0P}. This magnetization, M_P, about as large as can be produced by the instrumentation, will decay during the relaxation period, E (M_E), with a minimum potential signal amplitude proportional to the difference in the equilibrium magnetization values at B_{0P} and B_{0E}, and thus to $B_{0P} - B_{0E}$, which is never less than half B_{0P}.

The second FC sequence, call "pulse-up" (Fig. 2B), is used when B_{0E} is relatively high; more specifically, for $B_{0E} > B_{0P}/2$. The "soak field" is kept near zero during P for "pulse-up". In this mode, M_E will grow during E, with a minimum potential signal amplitude again proportional to $B_{0P}/2$. Thus, with either cycling protocol, the sensitivity of the relaxometer is related to the maximum magnitude of B_{0P}.

The FC relaxometer is superior to the standard tunable spectrometers in many aspects. The magnetic field can go down as low as 10 kHz, and even lower, with good accuracy by careful calibration and special attention to detail. It takes advantage of the strong nuclear magnetization and the elevated Larmor frequency under high-field conditions, and virtually eliminates sensitivity problems without influencing the phenomena occurring during the relaxation period. It is rather easy to obtain the desired frequency dependence with signal detection at one single field and no need for tuning the spectrometer.

Practically, with the FC technique one can measure water proton longitudinal relaxation rates rapidly and accurately at any field in the range 0.01–50 MHz, permitting the experimental determination of an NMRD profile to be compared with theoretical expectations (see Fig. 1).

E. THE CASE OF $Cu(OH_2)_6^{2+}$: THE SIMPLEST EXAMPLE OF WATER PROTON–UNPAIRED ELECTRON COUPLING

The proton longitudinal relaxation rates of deoxygenated pure water at 25°C are about 0.3 s^{-1} and are field-independent between 0.01 and 600 MHz [40,42,44,45]. The relaxation mechanisms of water protons in pure water are well understood [7,40,46]. The major contributions come from intra and inter molecular dipolar interactions between protons [46]. The intramolecular interaction is modulated by rotation and the intermolecular interaction is modulated by translational diffusion. Both these correlation times for pure water are $\approx 3 \times 10^{-12}$ s at 25°C. The relaxation equation for the first contribution is analogous to eqn. (3) (and is non-dispersive over the whole magnetic field range because $\omega_I \tau_r \ll 1$), whereas that for the second con-

tribution contains the translational diffusion correlation time, τ_D, and is also non-dispersive.

When $Cu(H_2O)_6^{2+}$ is present, the water proton relaxation rates drastically increase [47,48]. The values for a millimolar solution (relaxivity values) are around 2.0 $mM^{-1}\,s^{-1}$ at low field and 0.58 $mM^{-1}\,s^{-1}$ at high field in the frequency scale of NMRD. Figure 3 shows the complete NMRD profile for hexaaqua copper(II) solutions obtained with an FC relaxometer [47,48], and after subtraction of the small diamagnetic water contribution. The data clearly show a dispersion centred at $\approx$10 MHz, which must correspond to an ω_s dispersion. The shape is very close to the theoretical expectations of Fig. 1. From the data, T_{1M}^{-1} can be obtained as follows:

$$T_{1p}^{-1} = T_{1obs}^{-1} - T_{1dia}^{-1} = f_m(T_{1M} + \tau_M)^{-1} \tag{5}$$

where T_{1obs} is the measured T_1 value, T_{1dia} is the T_1 of the blank (water or water with an analog diamagnetic solute), f_m is the molar fraction of water protons interacting with the metal ion (in this case $f_M = 1.2 \times 10^{-3}/111$ where 12 is the number of interacting protons in the hexaaqua ion, 10^{-3} is the molarity of $Cu(H_2O)_6^{2+}$ and 111 is the "molarity" of water protons in water), and τ_M is the lifetime of the water protons in the paramagnetic metal site [49,50].

τ_M is the first kinetic parameter we encounter in the analysis of water proton relaxation dispersions. When measuring water proton relaxation rates to obtain information on the metal ion–water proton interaction, we assume that the paramag-

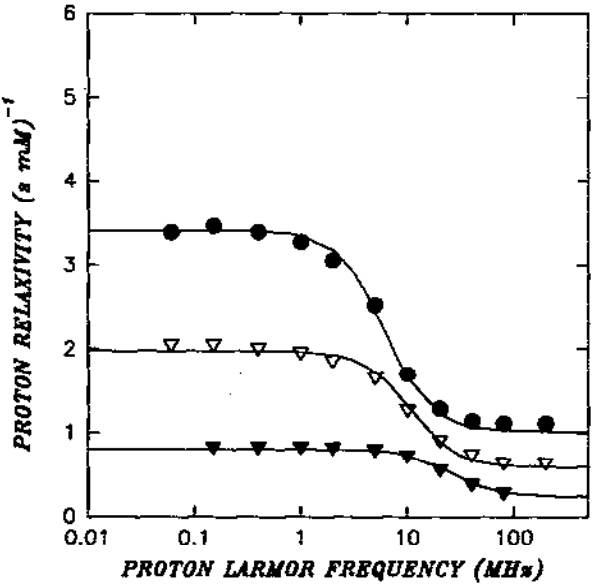

Fig. 3. Water ^1H NMRD profiles of $Cu(OH_2)_6^{2+}$ solutions at 5 (●), 25 (▽) and 65 (▼) °C [47]. The full lines represent the best fitting of the data to eqn. (3). The fitting parameters are: $r = 270$ pm; $\tau_r = 40$ (5°C), 26 (25°C) and 9.5 (65°C) ps.

netic effects caused by the nearby unpaired electron on nuclear relaxation rates are "propagated" evenly and in a short time over all the water proton spin system [51]. Propagation occurs by means of chemical exchange if chemical exchange occurs at a rate faster than T_{1M}^{-1} (i.e. the lifetime of a water proton in the paramagnetic site, τ_M, is shorter than T_{1M}). Then, we have a mean water proton relaxation rate which is the weighted average between the very fast relaxation rate in the paramagnetic site and the slow relaxation rate of bulk water. If τ_M is not negligible compared with T_{1M}, propagation is not complete and the paramagnetic effect measured on the bulk water signal starts being reduced. In the slow exchange situation ($\tau_M \gg T_{1M}$), T_{1M} is no longer experimentally accessible from measurements on the bulk water proton signal. The paramagnetic effect is quenched by τ_M, and eventually reduces to zero for the limiting situation where exchange does not occur. In principle, in this case, T_{1M} could be measured directly on the bound water signal, which should be observed separately from the bulk water signal because it is shifted by the additional magnetic field caused by the paramagnetic centre [52]. In practice, however, for diluted aqua ion solutions the signal is small and may be undetectable because it is too broad. It should be recalled that the paramagnetic broadening is proportional to T_{2M}^{-1} ($\Delta\nu = T_{2m}^{-1}/\pi$) and that the relation $T_{2M}^{-1} \geqslant T_{1M}^{-1}$ always holds [53].

Under slow exchange situation, NMRD gives immediate information on the lifetime of the bound water protons. Interestingly, this may or may not correspond to the lifetime of the coordinated water molecule. In several cases, NMRD has indeed demonstrated that protons may exchange with bulk water independently of the breaking of the metal–oxygen coordination bond [51] (see Sect. H).

A computer fitting of the data of Fig. 3 to eqns. (3) and (5) is shown in Fig. 3. As anticipated by comparing Figs. 1 and 3, the agreement is quite good. Apparently, eqn. (3) describes well the hexaaqua copper(II) system. The fitting parameters are: $r = 0.27$ nm, $\tau_c = 26$ ps at 25°C [48]. Thus, from a single NMRD profile we obtain reliable estimates of the metal–water proton distance, r (if the hydration number is known, as in this case), and the correlation time, τ_c. In this case, the water proton lifetime, τ_M, turns out to be small compared with T_{1M} ($T_{1M} = 4.5 \times 10^{-6}$ s at low field) [48]. Its estimate is therefore not possible. However, we can safely consider T_{1M} as a conservative upper limit for τ_M. The last parameter, τ_c, is the correlation time for the modulation of the electron–nucleus interaction. As anticipated in Sect. B, it is given by

$$\tau_c^{-1} = \tau_r^{-1} + \tau_s^{-1} + \tau_M^{-1} \tag{6}$$

i.e. the rate at which the interaction is modulated is the sum of the rates for the single processes of molecular rotation, electron relaxation and chemical exchange. Here is thus contained important information on the dynamics of the system. None of the above processes is faster than 2.6×10^{-11} s. The ESR spectrum of copper(II) is detectable at room temperature, so that a value of τ_s^{-1} of 3×10^9 s^{-1} can be estimated [53–55]. Although we have shown that τ_M is much shorter than 10^{-6} s,

chemical intuition argues against a proton exchange process on a timescale as short as 2.6×10^{-11} s. Here one can take advantage of the change in time scale produced by a different choice of resonating nucleus, and perform relaxation measurements on $H_2{}^{17}O$, which obviously give a much shorter T_{1M}^{-1}. A recent estimate yields $\tau_M = 2.3 \times 10^{-10}$ s [56]. τ_r is therefore dominating in this situation. A rotational correlation time of 2.6×10^{-11} s is in good agreement with estimates using the Stokes–Einstein equation [57–60].

$$\tau_r = \frac{4\pi r^3 \eta}{3kT} \tag{7}$$

according to which the rotational correlation time of a spherical molecule is proportional to its volume and to the viscosity of the solution, and inversely proportional to temperature.

F. $S > 1/2$ IONS

A τ_r of $\approx 3 \times 10^{-11}$ s at room temperature is indeed typical of aqua ions [51]. Yet, the NMRD profiles for other aqua ions can be completely different. This is the case, for instance, for $Co(H_2O)_6^{2+}$, which shows a very low, field-independent relaxivity (Fig. 4) [10,48]. Obviously, in this case, τ_c is much shorter than in the copper case, and therefore must be dominated by τ_s (eqn. (6)). From the absence of a

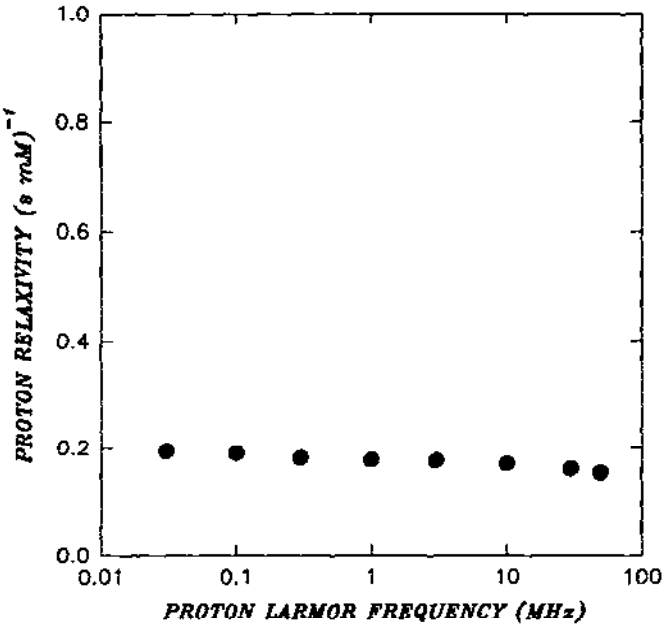

Fig. 4. Water ^1H NMRD profile of a $Co(OH_2)_6^{2+}$ solution at 25°C [48].

dispersion up to $\approx$ 100 MHz, an upper limit for τ_s of 10^{-11} s can be estimated. By assuming six regularly coordinated water molecules, a τ_c value at room temperature can be estimated and is ca. 3×10^{-12} s from eqn. (3) [48]. NMRD is thus a convenient way of estimating electron relaxation times in those cases where they are too short to be directly accessible using other techniques.

Another interesting example is provided by $Mn(H_2O)_6^{2+}$ [10,61,62]. It is known that Mn^{2+} has rather long electronic relaxation times, and therefore should behave like Cu^{2+}. On the other hand, Fig. 5 shows that the NMRD profile for $Mn(H_2O)_6^{2+}$ is strikingly different from both the copper(II) and cobalt(II) cases. In this case, it has been demonstrated that contact interactions are not negligible [10,47]. The correlation time for contact interaction, at variance with eqn. (6), only depends on τ_s and τ_M because contact interaction is rotationally invariant. Therefore, if both τ_s and τ_M are much longer than τ_r, contact interaction may become important at low field. The equation for contact interaction is [8,9]

$$T_{1M}^{-1} = \frac{2}{3} S(S+1)\left(\frac{A_c}{\hbar}\right)^2 \frac{\tau_c}{1+\omega_s^2\tau_c^2} \tag{8}$$

where $A_c/\hbar$ is the hyperfine coupling constant. The other symbols have the same meaning as in eqn. (3). It is apparent, therefore, that Fig. 5 shows the superposition of a contact and a dipolar contribution, the first having τ_s and the second τ_r as correlation time. In this case, the NMRD profile is even richer in information. The

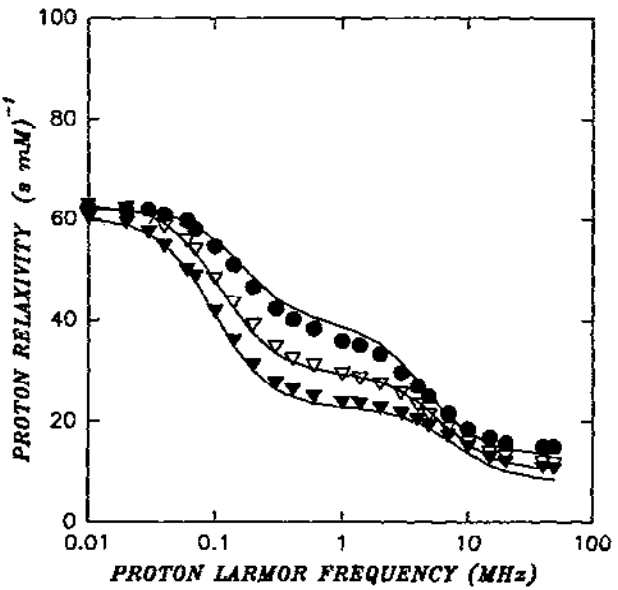

Fig. 5. Water ^{1}H NMRD profiles of $Mn(OH_2)_6^{2+}$ solutions at 5 (●), 15 (▽) and 25 (▼)°C [62]. The full lines are best fit curves calculated using eqns. (3) and (8) and the following parameters: $A_c/\hbar = 0.9$ MHz; $\tau_r = 55$ (5°C), 40 (15°C), 30 (25°C) ps; $\tau_s = 1.5$ (5°C), 2.2 (15°C), 2.5 (25°C) ns are obtained.

analysis of the data is quite complex, because it involves more parameters, but it proves successful [61,62]. The best fit parameters are listed in the caption of Fig. 5. Especially reliable values are obtained by analyzing the data simultaneously at different temperatures and using the temperature dependence of τ_r predicted by eqn. (7) [62] (see Sect. H).

As a further example of the variety of behaviour observed in the NMRD profiles of aqua ions, Figs. 6 and 7 show the profiles for $Ni(OH_2)_6^{2+}$ [63,64] and $Fe(OH_2)_6^{3+}$ [65,66]. In the first case, the profile is almost flat to relatively high field where it curves downwards, as expected for the beginning of a dispersion, but then raises abruptly and very soon surpasses the low-field value. Analogously, in the $Fe(OH_2)_6^{3+}$ profile, after a regularly shaped dispersion, an increase is apparent at high field.

It is now well established that the increase in relaxivity at high field, in these and other cases, is due to a field-dependence of τ_s [11,67–69]. This brings us closer to the essence of the electron-relaxation phenomenon: as for nuclei, electrons are relaxed by coupling with magnetic field fluctuations in the lattice and, depending on the particular phenomenon involved, these fluctuations may be characterized by a correlation time, τ_v. If τ_v is in the proper range, it originates a dispersive behaviour in the field dependence of the electron T_1^{-1} values. When the latter dominates in τ_c^{-1} (eqn. (6)), then a dispersion in the electron relaxation rate is reflected in an increase in nuclear relaxivity. The fact that we can have experimental access, not

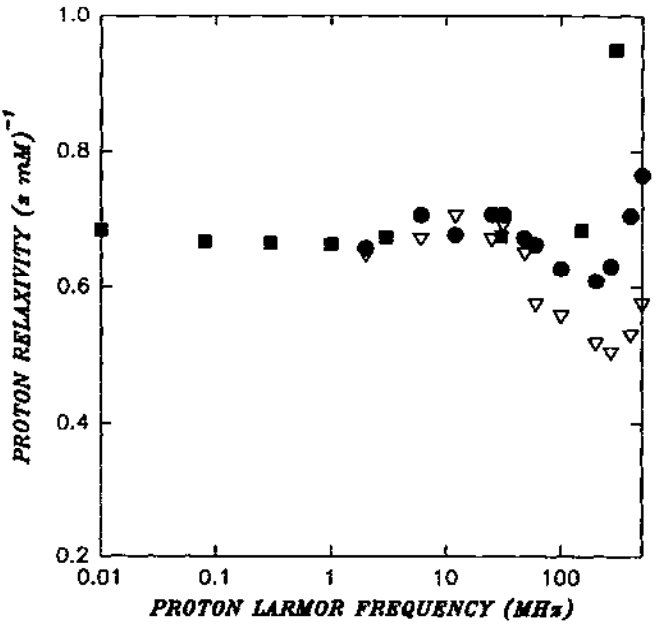

Fig. 6. Water ^1H NMRD profiles of $Ni(OH_2)_6^{2+}$ solutions at 25 (■), 51 (●) and 71 (▽)°C [48,64].

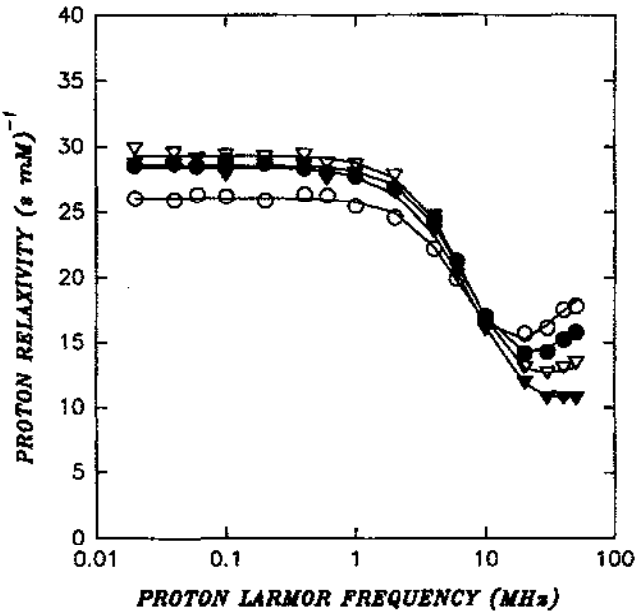

Fig. 7. Water ^{1}H NMRD profiles of $Fe(OH_2)_6^{3+}$ solutions at 5 (○), 15 (●), 25 (▽) and 35 (▼)°C [66]. The solid lines are the best fit curves calculated using eqns. (3), (8), and (12) and the best fit parameters are as follows: $A_c/\hbar = 1.2$ MHz; $\tau_r = 95$ (5°C), 68 (15°C), 51 (25°C), 40 (35°C) ps; $\tau_v = 7.8$ (5°C), 6.8 (15°C), 5.9 (25°C), 4.7 (35°C) ps; $\tau_M = 1.4$ (5°C), 0.91 (15°C), 0.58 (25°C), 0.49 (35°C) μs.

only to τ_s and τ_r, but also to τ_v provides a unique opportunity to test a hypothesis on how the various electron relaxation mechanisms work. It is very interesting, in this respect, to observe that all the main theories for electron relaxation in metal ion complexes date back to the 1940s and 1950s for solid state and to the 1960s for solutions, when EPR was systematically employed to analyze slow relaxing ions. Since then, the development has essentially stopped for the lack of new experimental tools. We are now in a position to advance this frontier of science further by using NMRD as the main investigation tool.

G. GENERALITIES ON ELECTRON RELAXATION MECHANISMS IN SOLUTION

Electron relaxation mechanisms are customarily divided into solid state and solution mechanisms [70,71]. The former are essentially described as due to the coupling between vibrational transitions occurring in the lattice and electronic transitions [13,72]. The coupling is allowed by the presence of spin–orbit coupling. Spin–orbit coupling is relatively small for metal ions of the first transition series and much more efficient for lanthanides, except gadolinium(III). At room temperature, the two main mechanisms are the so-called Van Vleck–Raman [73,74] and Orbach [74] mechanisms. In the Orbach mechanism, the electron spin system absorbs energy

from a vibrational transition undergoing a transition to an excited electronic state. In the transition, due to spin–orbit coupling, the system may also change spin state. Alternatively, the spin state may change when the electron returns to the ground state. Therefore, in the process, two energy quanta are exchanged, and their difference, which is very small, corresponds to the energy separation between the two spin states. This mechanism can be very efficient, yielding electron relaxation as short as 10^{-12} to 10^{-13} s provided low-lying (typically within thermal energies, i.e. a few hundred wavenumbers) electronic excited states exist [13,72]. The Van Vleck–Raman mechanism may be visualized as the simultaneous absorption and emission of the two energy quanta differing in energy of the appropriate amount. In this case, the presence of a low-lying excited state is no longer required (the system is said to be excited to a "virtual state"). However, the efficiency of this mechanism still depends on how close the electronic excited states are although, in this case, they may be as high as one or two thousand wavenumbers. The Van Vleck–Raman mechanism can account for electron relaxation times as short as 10^{-11} s [13,72]. Solid state mechanisms thus depend on the availability in the lattice of quanta of vibrational energy, called "phonons" in analogy with photons. In principle, a direct spin transition could also occur by absorption of a single, low-energy phonon [73,74]. In practice, however, this mechanism is very inefficient because phonons of such low energy are not nearly as abundant as thermal-energy phonons. Furthermore, the transition would be forbidden for Kramers ions if it were not for spin–orbit coupling, and the efficiency of the latter again depends on the admixture with excited states.

In solution there are electronic relaxation mechanisms which, by analogy with nuclei, can be described in terms of fluctuations of magnetic fields in the lattice [70,71,75]. Those which have been more extensively characterized are (a) modulation of g and A anisotropy due to rotation [76–80] and (b) modulation of quadratic zero field splitting [10,81,82]. Spin rotational mechanisms have also been described [83,84] but they are seldom relevant in the cases of interest here.

The first mechanism originates from the fact that the g factor can be anisotropic due to spin–orbit coupling. Hamiltonian (4) is then written in tensorial form:

$$\hat{\mathscr{H}} = \mu_B \mathbf{B}_0 \cdot \mathbf{g} \cdot \hat{\mathbf{S}} \tag{9}$$

Rotation of the molecules in solution produces a fluctuation of the magnetic moment associated with the molecule.

If the metal nucleus is magnetically active, the dipolar part of its interaction with the unpaired electron is also modulated by rotation, as described in Sect. C. The following term is added to the electron spin Hamiltonian:

$$\hat{\mathscr{H}} = \hat{\mathbf{I}} \cdot \mathbf{A} \cdot \hat{\mathbf{S}} \tag{10}$$

Finally, for $S > 1/2$, zero field splitting is also present, again due to the existence of spin–orbit coupling. Zero field splitting is described by the Hamiltonian.

$$\mathscr{H} = \hat{\mathbf{S}} \cdot \mathbf{D} \cdot \hat{\mathbf{S}} \tag{11}$$

and, again, modulation of the D tensor can induce relaxation. A static zero field splitting can be modulated by rotation [11]. In high-symmetry complexes, a transient zero field splitting may occur by instantaneous distortions of the coordination sphere caused, for example, by collision with solvent molecules [10].

H. ELECTRON RELAXATION IN AQUA IONS

As we have seen, electron relaxation in solution should be a function of the correlation time for the motion that modulates the electron lattice interaction. The motion, in turn, should be sensitive to the temperature and to the viscosity of the solution. Recording NMRD profiles as a function of temperature and/or viscosity should thus allow a better understanding of the electron relaxation mechanisms. The NMRD profiles of $Mn(OH_2)_6^{2+}$ solutions (Fig. 5) are particularly illustrative. By increasing temperature, it can be clearly seen that the dipolar contribution decreases and the relative dispersion shifts to high field, whereas the contact contribution increases and the relative dispersion shifts to low field [62]. Equation (3) fully accounts for the behaviour of the dipolar contribution. The correlation time is τ_c, and τ_r depends on temperature (and viscosity, which also strongly depends on temperature) as shown by eqn. (7). When the temperature increases, τ_r decreases and the experimental behaviour is accounted for. On the other hand, the contact interaction is a function τ_s. The experimental data show that τ_s increases with temperature [62].

It is proposed that, for $Mn(OH_2)_6^{2+}$, electron relaxation could arise from modulation of the quadratic zero field splitting brought about by collision with solvent molecules, according to the following equation due to Bloembergen and Morgan [10,82]:

$$\tau_s^{-1} = B^2 \left(\frac{\tau_v}{1 + \omega_s^2 \tau_v^2} + \frac{4\tau_v}{1 + 4\omega_s^2 \tau_v^2} \right) \tag{12}$$

where B^2 is proportional to the instantaneous quadratic zero field splitting and τ_v is the correlation time for the collision with solvent molecules.

A meaningful test of this proposal comes from NMRD profiles recorded at increasing viscosity [61,62]. The solution viscosity can be increased by adding ethylene glycol or glycerol. The behaviour is shown in Fig. 8 [61]. In short, the increase in viscosity causes an increase of τ_r (eqn. (7)) and τ_v, and should thus cause an increase of the dipolar contribution and the decrease and disappearance of the contact contribution. The information on τ_s from the contact contribution is then lost, but is regained from the dipolar contribution because very soon τ_s becomes shorter than τ_r and therefore dominates the correlation time τ_c (eqn. (6)). The increase of relaxivity at high field witnesses the beginning of the $\omega_s \tau_v$ dispersion (eqn. (12)). Therefore, B^2 and τ_v can be separately evaluated, and the value of τ_v in pure water easily extrapolated to $\approx 6 \times 10^{-12}$ s [62]. That the value of τ_v is of general validity

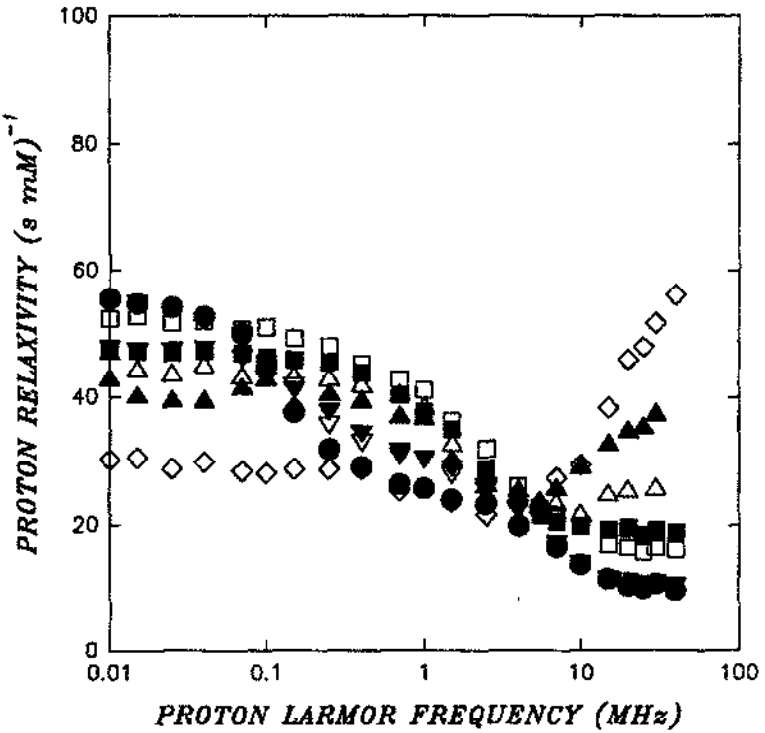

Fig. 8. Water ^{1}H NMRD profiles of $Mn(OH_2)_6^{2+}$ solutions at 13°C in pure water (●) and with increasing amounts of d_5-glycerol: 10% (▽), 20% (▼), 35% (□), 45% (■), 55% (△), 65% (▲), 75% (◇) [61].

is demonstrated by the analysis of the $Ni(OH_2)_6^{2+}$ (Fig. 6) [63,64] and $Fe(OH_2)_6^{3+}$ (Fig. 7) [65,66] data, where the increase of relaxivity at high field is already observed in pure water. The instantaneous zero field splitting induced by solvent bombardment increases from Mn^{2+} to Fe^{3+} to Ni^{2+} because the spin–orbit coupling effects increase [67]. Therefore, τ_s becomes shorter and shorter and for Ni^{2+}, even in pure water, it dominates τ_c. We would like to point out that, in the case of $Fe(OH_2)_6^{3+}$, the water residence time is known to be around 3×10^{-4} s [51]. The observation of relatively fast proton exchange ($\tau_M = 6 \times 10^{-7}$ s at 25°C) [65,66] demonstrates that water protons can exchange without detachment of the water oxygen from the coordination sphere.

The above examples should serve the purpose of illustrating how NMRD can be exploited to obtain dynamic information of a different kind. Recent experiments are allowing a deeper understanding of the electron relaxation mechanisms for many other metal ions including VO^{2+} [85], Ti^{3+} [86], and Gd^{3+} [42].

Present knowledge about the electronic relaxation mechanisms operative in aqua ions is summarized in Table 1. Fast-relaxing ions such as lanthanides or Co^{2+} apparently have a field-independent τ_s. This means that either the correlation time

TABLE 1
Electronic relaxation mechanisms of some aqua ions of transition metals [87]

Aqua ion	Main relaxation mechanism	Room temperature τ_s at low field (at 25°C) (s)	Field dependence (at 25°C) (s)	Ref.
$Ti(OH_2)_6^{3+}$	Orbach	4×10^{-11} (20°C)	None	86
$VO(OH_2)_5^{2+}$	A-anisotropy	4.0×10^{-10}	$\tau_v = 6 \times 10^{-12}$	85
$Mn(OH_2)_6^{2+}$	ZFS	3.5×10^{-9}	$\tau_v = 5.3 \times 10^{-12}$	10,62
$Fe(OH_2)_6^{3+}$	ZFS	8.4×10^{-11}	$\tau_v = 5.9 \times 10^{-12}$	60,61
$Co(OH_2)_6^{2+}$	Orbach	3.0×10^{-12}	None	48
$Ni(OH_2)_6^{2+}$	ZFS	3.0×10^{-12}	$\tau_v = 2.2 \times 10^{-12}$	63,64
$Cu(OH_2)_6^{2+}$	Raman[a]	3.0×10^{-10}	None	47,55,56,88
$Gd(OH_2)_9^{3+}$	ZFS	1.3×10^{-10}	$\tau_v = 1.6 \times 10^{-11}$	42,48,49
$Ln(OH_2)_9^{3+}$	Orbach	$10^{-12} - 10^{-13}$	None	6,43,90,74,91

[a]Orbach and spin-rotation mechanisms may not be negligible [6,92].

τ_v is too short to make τ_s field-dependent in the accessible field range, or that mechanisms of the solid state type, which cannot be conveniently described in terms of fluctuations, are operative. In a broad sense, this may not be a dilemma between two physically different mechanisms but rather between two different approaches to describe the same phenomenon. Indeed, if we exclude modulation of A-anisotropy, all other electron relaxation mechanisms, both in the solid state and in solution are somehow linked to the presence of spin–orbit coupling [6]. Solid-state type mechanisms can actually be operative in solution [92]. For lanthanides and Co^{2+}, the mechanism should be of the Orbach type, given the availability of low-lying excited states [48,68]. It has been recently confirmed that relaxation of $Ti(OH_2)_6^{3+}$ is likewise accounted for by an Orbach mechanism [86]. On the other hand, we have seen that relaxation of Mn^{2+} [10,61,62], Fe^{3+} [65,66] and Ni^{2+} [63,64] can be accounted for by fluctuations in the quadratic zero field splitting. τ_v corresponds here to the correlation time for geometrical distortions of the complex caused by collision with solvent molecules*. Interestingly, relaxation of VO^{2+}, which is an $S = 1/2$ ion and therefore has no zero field splitting, is also governed by a τ_v which is very similar in magnitude to that involved in relaxation of Mn^{2+}, Fe^{3+}, and Ni^{2+}. This has been interpreted in terms of modulation of the hyperfine coupling tensor with the metal nucleus.

One could expect that the same mechanism could be operative for $Cu(OH_2)^{2+}$. Instead, as we have shown, τ_s for Cu^{2+} is irrelevant in the NMRD and is probably

* The somewhat shorter τ_v value estimated for Ni^{2+} and the longer value estimated for Gd^{3+} cannot be easily explained. More accurate estimates should be obtained before attempting a justification of the difference.

field-independent. A Raman-type relaxation mechanism could account for the relaxation of the aqua ion [45,53,54,88]. The situation is different for tetragonal copper complexes, which have far higher excited states and therefore longer τ_s [6,43,68]. In these cases, the dominant mechanism in solution could be modulation of hyperfine coupling as in the VO^{2+} case [85]. However, analysis of macromolecular systems (see below) shows that this is not likely to be the case.

I. MACROMOLECULAR SYSTEMS

Increasing interest in the role of metal ions in biological macromolecules (see the review by Bertini in this volume) has also produced, in the past ten years, an extensive set of NMRD data on paramagnetic metalloproteins and metalloenzymes [6,67–69]. From the point of view of the understanding of the phenomenon of electron relaxation in general, the presence of a macromolecule is a distinctive advantage because τ_r is long (typically $\geqslant 10^{-8}$ s for a 30 kD protein) and therefore always leaves τ_s as the major contributor to the correlation time. In this way, systems with long τ_s can be directly investigated. Again, the phenomena responsible for the shapes of the NMRD curves are far richer than expected. To start again with copper as the simplest example, Fig. 9 shows the NMRD profile of copper(II) superoxide dismutase [93], a 32 kD dimer containing one copper(II) and one zinc(II) ion in each of the two identical subunits. The profile is clearly different from whatever behaviour has been encountered so far. More or less striking deviations from the Solomon–Blombergen–Morgan behaviour are observed for VO^{2+} [94], Co^{2+} [95], and Mn^{2+} -containing proteins [96] (Figs. 10–12). The task of rationalizing these profiles theoretically was undertaken in our laboratory some years ago [95,97–104]. We have now derived appropriate equations that should substitute for the Solomon equation in macromolecules: a detailed description of the approach is out of place here, but we think it useful to explain the physical origin of the deviation.

In real systems, the spin Hamiltonian describing the electron spin is always Hamiltonian (9), to which Hamiltonian (10) should be added when the metal nucleus has a nuclear spin, and Hamiltonian (11) should be added when $S > 1/2$. Under these conditions, ω_s in eqn. (3) is no longer the electron spin Larmor frequency, which is a constant for a given magnetic field, but may be of the order of $A/\hbar$ or $D/\hbar$ and be strongly orientation-dependent. If this is properly taken into account in the derivation of eqn. (3), completely different NMRD profiles are predicted [6]. The data in Fig. 9 [98] and Fig. 10 [94] are fitted with computer programs that include the effect of Hamiltonian (10) and, noticeably, a field-independent τ_s, the data in Fig. 11 are fitted with an equation that includes Hamiltonian (11) and, again, a field-independent τ_s [95], and the data in Fig. 12 with a numerical procedure that includes the effects of Hamiltonian (11) and a field-dependent τ_s according to eqn. (12) [99]. Attention should be drawn to the fact that τ_v is $\approx 5 \times 10^{-11}$ s, i.e. about one order of magnitude longer than in the aqua ion [99].

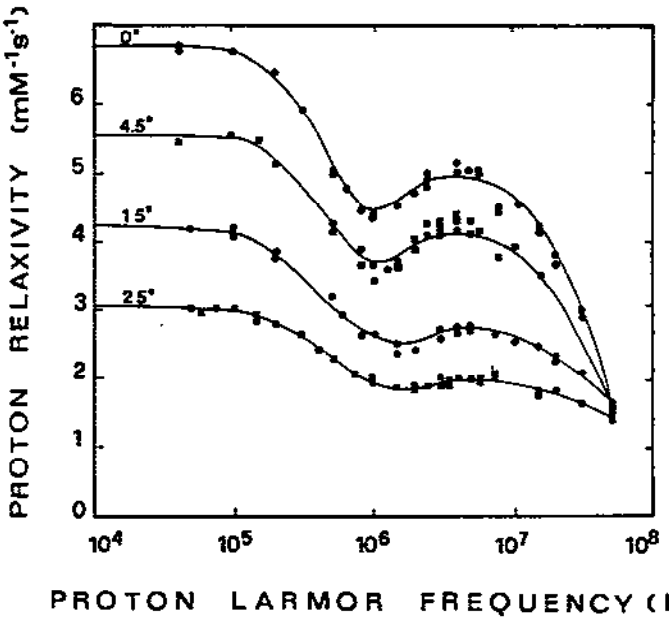

Fig. 9. Water ^{1}H NMRD profiles of Cu_2Zn_2SOD solutions at various temperatures [93]. The solid lines represent the calculated curves with inclusion of Hamiltonian (10) by using the following parameters: $A_\parallel = 137 \times 10^{-4}$, $A_\perp = 40 \times 10^{-4}$ cm^{-1}, $r = 325$ pm (assuming one interacting water, $\tau_s = 4.6$ (0°C), 3.8 (4.5°C), 2.5 (15°C), 1.8 (25°C) ns. and angle, θ, of 20°, between the average metal–proton vector and the molecular z axis.

From the analysis of these and other NMRD data on paramagnetic macromolecules, some general and perhaps unexpected features of electron relaxation mechanisms start to appear. Fast-relaxing metal ions such as Co^{2+} and lanthanides essentially maintain the same electronic relaxation times on passing from small aqua ions [46] to macromolecules [43,95], and the same as those measured in a solid crystal lattice [6,68]. Surprisingly, even ions such as Cu^{2+}, which relax much more slowly, turn out to relax with similar rates in small complexes and in macromolecules [88], and, again, similar to the rates observed in the solid state [13]. Other ions such as Ni^{2+} and Mn^{2+} have sizably different electronic relaxation rates in macromolecules with respect to small complexes [43,68]. This can be ascribed, as we have seen, to the change in τ_v. Even more surprisingly, in no case is a dramatic decrease in efficiency of the electronic relaxation mechanism with increasing molecular weight observed as should be expected for those mechanisms which depend on τ for modulation. Apparently, even for small molecules where rotational mechanisms may be dominant, other mechanisms not modulated by rotation and not much less efficient must be present, so that an increase in molecular weight does not have a dramatic effect. Non-rotational mechanisms may be either of a solid-state type or of the τ_v -modulated type.

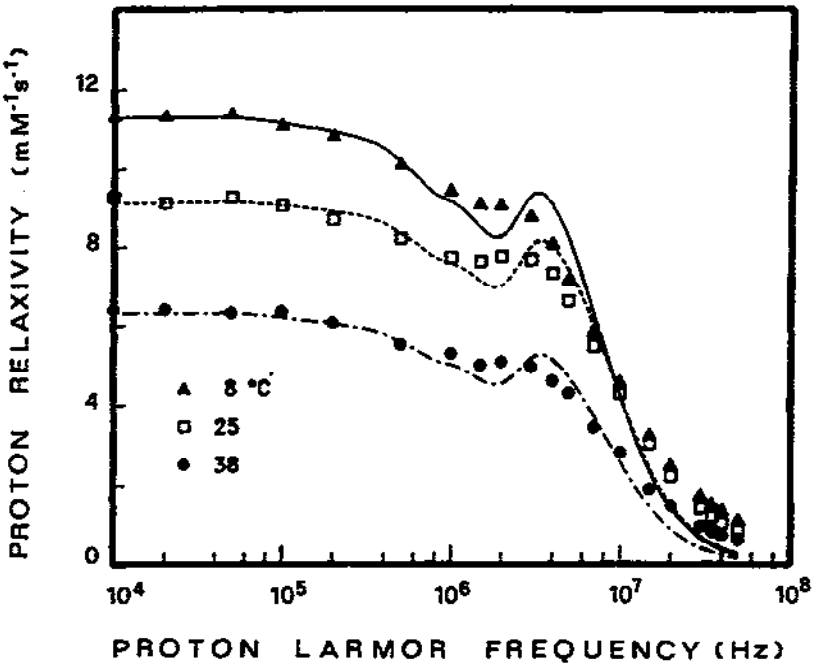

Fig. 10. Water ^{1}H NMRD data of Bisoxovanadium(IV) transferrin at (▲) 8°C, (□) 25°C, and (●) 38°C [94]. The lines through the data points represent the calculated curves with inclusion of Hamiltonian (10) by using the following parameters: $A_{\parallel} = 170 \times 10^{-4}$ cm^{-1}, $A_{\perp} = 60 \times 10^{-4}$ cm^{-1}, $r = 370$ pm (assuming one interacting water), $\tau_s \approx 20$ ns and $\theta \approx 30°$.

This observation allows us to speculate further on the intimate nature of the electron relaxation phenomenon. The fact that solid state mechanisms are totally maintained in solution means that the "phonon" picture is not restricted to solids [13,70–72]. As a matter of fact, on the time scale of phonon dynamics, a liquid is a solid, in the sense that many sound waves can travel back and forth over the sample, with the associated atomic displacements about the equilibrium position, before a solvent molecule can actually travel an appreciable distance. Therefore, besides the algebraic difficulty in translating the relaxation equations of the solid state to make them quantitatively applicable to solutions [92], the relaxation mechanisms are maintained, and we can think of a metal ion complex with its cage of solvent molecules as a microcrystal. A conceptual link can be actually provided by macromolecules, which can be more easily visualized as microcrystals. To this end, τ_v cannot obviously be related to solvent collision rate, and, indeed, τ_v in macromolecules is much longer. Its meaning is more probably related to the presence of fluctuations of relatively slower frequency than those present in a small molecule. By using again the language of solid state theory, the distribution of phonon frequencies in a crystal range from infrared frequencies (proportional to the reciprocal of interatomic distances) to very low frequencies, which extend as low as the reciprocal

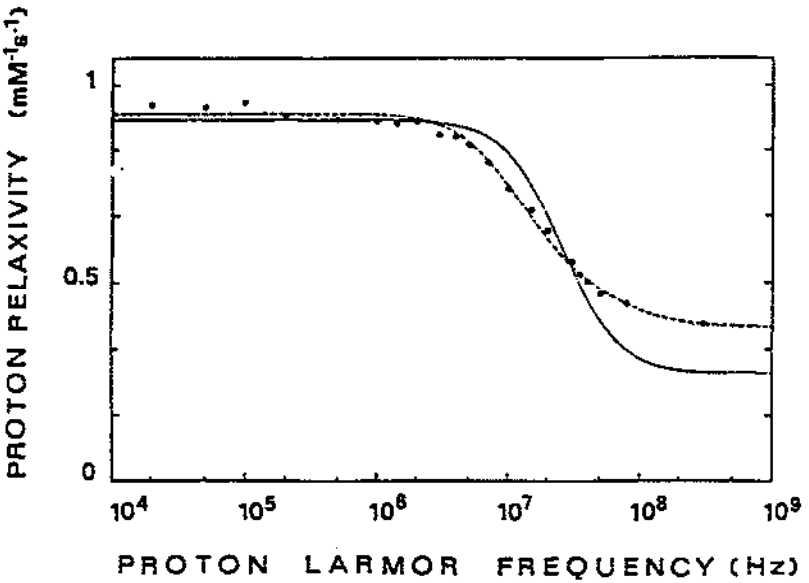

Fig. 11. Water ^{1}H NMRD profiles of cobalt(II) substituted human carbonic anhydrase I at pH = 9.9 [95]. The data are fitted with (broken line) and without (solid line) the inclusion of Hamiltonian (11). The best fit parameters for the former case are: $\tau_c = 33$ ps, $r = 270$ pm (assuming one interacting water), $\theta = 72°$.

of the macroscopic crystal dimension. If a metal complex is viewed as a microcrystal, its radius increases by about one order of magnitude on passing from aqua ions to macromolecules of ≈ 30 kD, thereby increasing the range of low frequencies available by one order of magnitude. This picture would be consistent with the order of magnitude increase in τ_v experimentally observed. Recent advances in molecular dynamics simulations show that many interesting dynamic phenomena in proteins occur at the time scale of τ (10–100 ps) [105]. These fluctuations may play a role in lowering the energy barriers of the various steps of catalytic pathway in enzymes [105], especially when multiple interactions between the enzyme and a complex substrate are required. This new way of looking at enzyme–substrate interactions could be termed hand and glove as a modification of the famous lock and key concept [106].

J. PERSPECTIVES

While briefly summarizing the various types of information that can be obtained through NMRD measurements on paramagnetic systems, we will attempt to provide a feeling for the perspectives in the applications. We have seen that water proton NMRD can give information on the time constants for various dynamic processes.

One of them is the electronic relaxation time. Understanding its field, temperature and viscosity dependences reveal the nature of the electron relaxation mecha-

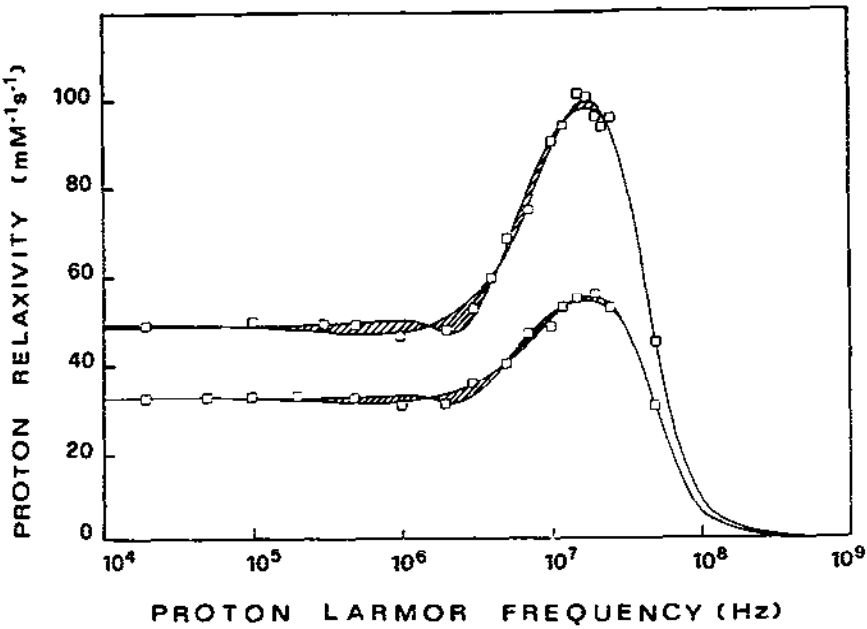

Fig. 12. Water ^{1}H NMRD profiles of Mn(II) concanavalin. A solution at 25 and 5°C [96]. The solid curves are calculated by with (upper line at 0.7 MHz) or without (lower line at 0.7 MHz) zero field splitting. The best fit parameters are: 25°C, $D = 0\ cm^{-1}$: n (number of protons at 280 pm from the metal) = 15.3, $\tau_M = 1.3\ \mu s$, $\tau_v = 69\ ps$, $\tau_r = 87\ ns$; $D = 0.04\ cm^{-1}$: $n = 6.6$, $\tau_M = 0.47\ \mu s$, $\tau_v = 44\ ps$, $\tau_r = 20\ ns$, $\theta = 24°$; 5°C, $D = 0\ cm^{-11}$: $n = 13.3$, $\tau_M = 21\ \mu s$, $\tau_v = 66\ ps$, $\tau_r = 120\ ns$; $D = 0.04\ cm^{-1}$: $n = 6.3$, $\tau_M = 0.89\ \mu s$, $\tau_v = 38\ ps$, $\tau_r = 28\ ns$, $\theta = 38°$.

nism operative in the system. In turn, these mechanisms provide information on the electronic structure. From the dynamic point of view, we learn about the motions in the lattice that modulate the electron–lattice coupling. In many cases, chemical exchange rates can be also measured.

One area of application where water proton NMRD has been extremely successful is the analysis of metal hydration in paramagnetic metalloproteins or metalloenzymes [43,69,107,108]. Hydrolytic metalloenzymes often perform their task by activating a water molecule through coordination at the active site metal, and by providing hydrogen bonds with protein residues for further lowering the water pK_a [109]. The coordinated water then ionizes to a coordinated hydroxide which performs nucleophilic attack on the substrate. Even if the native metal is diamagnetic, often a paramagnetic metal can be substituted for the native metal without abolishing the enzymatic activity [110]. The hydration of the metal can then be studied by NMRD. Knowing the hydration state of the metal ion under a variety of conditions (pH, presence of inhibitors, substrates or pseudo-substrates) and the lifetime of the coordinated species is thus of fundamental importance in understanding the various steps of the catalytic mechanism [109].

Another area where nuclear magnetic relaxation studies provide unique information is in the understanding of the phenomenon of magnetic coupling among paramagnetic metal centres in polymetallic systems. These systems are receiving much attention today either because of their sometimes interesting macroscopic magnetic properties or because they are more and more frequently discovered at the active centre of metalloproteins and metalloenzymes [102]. Biological redox reactions often involve such species. Whereas magnetic susceptibility measurements give information on the total spin state and susceptibility of the cluster, by monitoring the nuclear relaxation and shift properties of individual nuclei selectively interacting with one or another metal ion in the cluster, selective information is obtained on the spin state and relaxation times of the individual metal ions [111]. Quantitative information can also be obtained on the shortening of the electronic relaxation time of a slow-relaxing metal ion due to magnetic coupling with a fast-relaxing metal ion [111], and on the additional electron relaxation mechanisms which arise by the presence of more than two metal ions coupled together [6].

One of the most striking applications of the nuclear relaxation properties of paramagnetic systems is in the field of contrast agents in magnetic resonance imaging (MRI) [42]. In the past ten years, MRI has become very widespread as X-ray techniques in obtaining images for clinical purposes. The two obvious advantages over X-ray are the elimination of the risks associated with high-energy radiation and the dramatic increase in resolution and quality of images of soft tissues, especially brain and bone marrow [112]. In MRI, contrast is achieved by differentiating the water proton resonances from the various parts of the sample on the ground of their T_1 and T_2 values. Contrast can be greatly enhanced by the use of paramagnetic substances (contrast agents) that can be selectively transported to the desired portions of the tissue. Obviously, toxicity problems are always reduced proportionally to the reduction of the clinical dose of a given substance, and therefore it is important to look for the most efficient relaxing agents on a relaxivity basis. From what we have discussed in the previous sections, NMRD proves indispensable in planning more and more efficient contrast agents [42,113–115]. We have seen that Mn^{2+} and Gd^{3+}. are the most efficient relaxation reagents. We now understand how their efficiency is optimal for the magnetic fields used in MRI (usually around 20 MHz ^1H resonance frequency) because of the field dependence of the electronic relaxation time. We know that the efficiency can be increased by increasing the rotational correlation time. Shift reagents can thus be planned where a metal ion such as Mn^{2+} and Gd^{3+}, is bound to a macromolecule [116] (often a protein, but also colloidal particles of different nature are currently being tested [42]) or where small metal ion complexes are polymerized to increase the molecular weight and the number of relaxation centres at the same time [116].

It is the hope of the authors that this account of a research field, which may not be as familiar to coordination chemists as other subjects covered in this volume, at least succeeded in conveying a message: here we are building a technique and a

body of theories which touch on very fundamental physical concepts, and at the same time allow a wealth of applied research of unquestionable usefulness for mankind. This is how we think science should be in today's world. We do believe, as Luigi Sacconi taught us, that basic research is indispensable for the progress of science. But we also believe that (a) basic research could, and should, be oriented where the demand from applied research is higher, and (b) applied chemical research should be as basic as basic research in terms of depth of scientific understanding, or else it easily falls back into alchemy.

REFERENCES

1 L. Sacconi and R. Cini, J. Chem. Phys., 18 (1950) 1124.
2 L. Sacconi and R. Cini, J. Am. Chem. Soc., 76 (1954) 4239.
3 L. Sacconi, P. Paoletti and R. Cini, J. Am. Chem. Soc., 80 (1958) 3583.
4 E. Frasson, C. Panattoni and L. Sacconi, J. Phys. Chem., 63 (1959) 1908.
5 L. Sacconi, R. Cini, M. Ciampolini and F. Maggio, J. Am. Chem. Soc., 82 (1960) 3487.
6 L. Banci, I. Bertini and C. Luchinat, Nuclear and Electron Relaxation, The Electron Nucleus Hyperfine Coupling in Diluted Systems, VCH, Weinheim, 1991.
7 I. Solomon, Phys. Rev., 99 (1955) 559.
8 I. Solomon and N. Bloembergen, J. Chem. Phys., 25 (1956) 261.
9 N. Bloembergen, J. Chem. Phys., 27 (1957) 572.
10 N. Bloembergen and L.O. Morgan, J. Chem. Phys., 34 (1961) 842.
11 J. Kowalewski, L. Nordenskiöld, N. Benetis and P.-O. Westlund, Prog. Nucl. Magn. Reson. Spectrosc., 17 (1985) 141.
12 L. Nordenskiöld, L. Laaksonen and J. Kowalewski, J. Am. Chem. Soc., 104 (1982) 379.
13 A. Abragam and B. Bleaney, Electron Paramagnetic Resonance of Transition Ions, Clarendon Press, Oxford, 1970.
14 S.H. Koenig and W.E. Schillinger, J. Biol. Chem., 244 (1969) 3283.
15 R.V. Pound, Phys. Rev., 81 (1951) 156.
16 M. Packard and R. Varian, Phys. Rev., 93 (1954) 941.
17 A. Bloom and D. Mansir, Phys. Rev., 93 (1954) 941.
18 G. Bènè, Arch. Sci., 10 (1957) 200.
19 A. Abragam and W.G. Proctor, Phys. Rev., 109 (1958) 1441.
20 R.T. Schumacher, Phys. Rev., 112 (1958) 837.
21 A.G. Anderson and A.G. Redfield, Phys. Rev., 116 (1959) 583.
22 P.S. Pershan, Phys. Rev., 117 (1960) 109.
23 A.G. Redfield, Phys. Rev., 130 (1963) 589.
24 B.C. Johnson and W.I. Goldberg, Phys. Rev., 145 (1966) 380.
25 G. Bènè, Arch. Sci., 18 (1965) 213.
26 H. Sprinz, Ann. Phys., 20 (1967) 168.
27 R. Hausser, H. Kolb and G. Siegle, Z. Angew. Phys., 22 (1967) 375.
28 A.G. Redfield, W. Fite and H.E. Bleich, Rev. Sci. Instrum., 39 (1968) 710.
29 G.P. Jones, J.T. Daycock and T.T. Roberts, J. Phys. E, 2 (1968) 630.
30 M. Minier, Phys. Rev., 182 (1969) 437.
31 Z. Florkowski, J.W. Hennel and B. Blicharska, Nucleonics, 14 (1969) 563.
32 R. Kimmich and F. Noack, Z. Angew. Phys., 29 (1970) 248.
33 B.F. Melton and V.L. Pollak, Rev. Sci. Instrum., 42 (1971) 769.
34 K. Hallenga and S.H. Koenig, Biochemistry, 15 (1976) 4255.

35 R. Blinc, M. Luzar, M. Mali, R. Osredkar, J. Seligar and M. Vilfan, J. Phys. (Paris) Colloq., 37 (1976) C3.
36 M. Stohrer and F. Noack, J. Chem. Phys., 67 (1977) 3729.
37 D.T. Edmonds, Phys. Rep., 29 (1977) 233.
38 E.V. Doldammer and W. Kreysch, Ber. Bunsenges. Phys. Chem., 82 (1978) 463.
39 D. Dally and W. Müller-Warmuth, Ber. Bunsenges. Phys. Chem., 82 (1978) 792.
40 F. Noack, Progr. Nucl. Magn. Reson. Spectrosc., 18 (1986) 171.
41 R.G. Bryant, R.D. Brown III and S.H. Koenig, Biophys. Chem., 16 (1982) 133.
42 S.H. Koenig and R.D. Brown III, Prog. Nucl. Magn. Reson. Spectrosc., 22 (1990) 487.
43 I. Bertini and C. Luchinat, NMR of Paramagnetic Molecules in Biological Systems, Benjamin/Cummings, Menlo Park, CA, 1986.
44 K. Krynicki, Physica, 32 (1966) 167.
45 V. Graf, F. Noack and G. Bènè, J. Chem. Phys., 72 (1980) 861.
46 N. Bloembergen, E.M. Purcell and R.V. Pound, Phys. Rev., 73 (1948) 679.
47 R. Hausser and F. Noack, Z. Phys., 182 (1964) 93.
48 L. Banci, I. Bertini and C. Luchinat, Inorg. Chim. Acta, 100 (1985) 173.
49 T.J. Swift and R.E. Connick, J. Chem. Phys., 37 (1962) 307.
50 Z. Luz and S. Meiboom, J. Chem. Phys., 40 (1964) 2686.
51 H.G. Hertz, in F. Franks (Ed.), Water: A Comprehensive Treatise, Vol. 3, Plenum Press, New York, 1973.
52 Z. Luz and R.G. Shulman, J. Chem. Phys., 43 (1965) 3750.
53 A. Abragam, The Principles of Nuclear Magnetism, Oxford University Press, Oxford, 1961.
54 W.B. Lewis, M. Alei and L.O. Morgan, J. Chem. Phys., 44 (1966) 2409.
55 S. Fugiwara and H. Hayashu, J. Chem. Phys., 43 (1965) 23.
56 D.H. Powell, L. Helm and A.E. Merbach, J. Chem. Phys., 95 (1991) 9258.
57 G. Stokes, Trans. Cambridge Philos. Soc., 9 (1956) 5.
58 A. Einstein, Investigations on the Theory of the Brownian Movement, Dover, New York, 1956.
59 P. Debye, Polar Molecules, Dover, New York, 1929.
60 R.T. Boere and R. Kidel, Annu. Rep. NMR Spectrosc., 13 (1982) 319.
61 S.D. Kennedy and R.G. Bryant, Magn. Reson. Med., 2 (1985) 14.
62 I. Bertini, F. Briganti, C. Luchinat and Z. Xia, J. Magn. Reson., in press.
63 H.L. Friedman, M. Holz and H.G. Hertz, J. Chem. Phys., 70 (1979) 3369.
64 J. Kowalewski, T. Larsson and P.-O. Westlund, J. Magn. Reson., 74 (1987) 56.
65 S.H. Koenig, C.M. Baglin, E. Goldstein and G.L. Wolf, Magn. Reson. Med., 2 (1985) 283.
66 I. Bertini, F. Capozzi, C. Luchinat and Z. Xia, J. Phys. Chem., submitted for publication.
67 I. Bertini, F. Briganti and C. Luchinat, in N. Niccolai and N. Valensin (Eds.), Advanced Magnetic Resonance Techniques in Systems of High Molecular Complexity, Birkhaüser, Boston, 1986.
68 L. Banci, I. Bertini and C. Luchinat, Magn. Reson. Rev., 11 (1986) 1.
69 I. Bertini, C. Luchinat and L. Messori, in H. Sigel (Ed.), Metal Ions in Biological Systems, Vol. 21, Dekker, Basle, 1987.
70 I. Bertini, C. Luchinat and G. Martini, Electron Relaxation (Theory), in Electron Spin Resonance Handbook, CRC Press, Boca Raton, FL, 1991.
71 I. Bertini, C. Luchinat and G. Martini, Electron Relaxation (Data Collection), in Electron Spin Resonance Handbook, CRC Press, Boca Raton, FL, 1991.
72 S. Geschwind, Electron Paramagnetic Resonance, Plenum Press, New York, 1972, p. 353.
73 J.H. Van Vleck, Phys. Rev., 57 (1940) 426.

74 R. Orbach, Proc. R. Soc. London Ser. A, 264 (1961) 458.
75 L.T. Muus and P.W. Atkins, Electronic Spin Relaxation in Liquids, Plenum Press, New York, 1972.
76 D. Kivelson, J. Chem. Phys., 33 (1960) 1094.
77 H.M. McConnell, J. Chem. Phys., 25 (1956) 709.
78 B.R. McGarvey, J. Chem. Phys., 61 (1957) 1232.
79 R.N. Rogers and G.E. Pake, J. Chem. Phys., 33 (1960) 1107.
80 G.V. Bruno, J.K. Harrington and M.P. Eastman, J. Phys. Chem., 81 (1977) 11.
81 H. Levanon, S. Charbinsky and Z. Luz, J. Chem. Phys., 53 (1970) 3056.
82 M. Rubinstein, A. Baram and Z. Luz, Mol. Phys., 20 (1971) 67.
83 P.W. Atkins and D. Kivelson, J. Chem. Phys., 44 (1966) 169.
84 G. Nyberg, Mol. Phys., 12 (1967) 69.
85 I. Bertini, C. Luchinat and Z. Xia, J. Magn. Reson., in press.
86 I. Bertini, C. Luchinat and Z. Xia, Inorg. Chem., 31 (1992) 3152.
87 I. Bertini, C. Luchinat and Z. Xia, in preparation.
88 I. Bertini, C. Luchinat, R.D. Brown III and S.H. Koenig, J. Am. Chem. Soc., 111 (1989) 3532.
89 S.H. Koenig and M. Epstein, J. Chem. Phys., 63 (1975) 2279.
90 B.M. Alsaadi, F.J.C. Rossotti and R.J.P. Williams, J. Chem. Soc. Dalton Trans., (1980) 2147.
91 P.D. Burs and G.N. La Mar, J. Magn. Reson., 46 (1982) 61.
92 D. Kivelson, J. Chem. Phys., 45 (1966) 1324.
93 B.P. Gaber, R.D. Brown III, S.H. Koenig and J.A. Fee, Biochim. Biophys. Acta, 271 (1972) 1.
94 I. Bertini, F. Briganti, S.H. Koenig and C. Luchinat, Biochemistry, 24 (1985) 6287.
95 I. Bertini, C. Luchinat, M. Mancini and G. Spina, J. Magn. Reson., 59 (1984) 213.
96 S.H. Koenig and R.D. Brown III, J. Magn. Reson., 61 (1985) 426.
97 I. Bertini, C. Luchinat, M. Mancini and G. Spina, in R.D. Willett, D. Gatteschi and O. Kahn (Eds.), Magneto-structural Correlations in Exchange-coupled Systems, Reidel, Dordrecht, 1985.
98 I. Bertini, F. Briganti, C. Luchinat, M. Mancini and G. Spina, J. Magn. Reson., 63 (1985) 41.
99 L. Banci, I. Bertini, F. Briganti and C. Luchinat, J. Magn. Reson., 66 (1986) 58.
100 I. Bertini, C. Luchinat and J. Kowalewski, J. Magn. Reson., 62 (1985) 235.
101 L. Banci, I. Bertini and C. Luchinat, Chem. Phys. Lett., 118 (1985) 345.
102 I. Bertini and C. Luchinat, in K.D. Karlin and J. Zubieta (Eds.), Biochemical and Inorganic Aspects of Copper Coordination Chemistry, Adenine Press, New York, 1986.
103 I. Bertini, L. Banci and C. Luchinat, in L. Que, Jr. (Ed.), Metal Clusters in Protein, ACS Symp. Ser. 372, American Chemical Society, Washington, DC, 1988.
104 I. Bertini, L. Banci, R.D. Brown III, S.H. Koenig and C. Luchinat, Inorg. Chem., 27 (1988) 951.
105 J.A. McCammon and S. Harvey, Dynamics of Proteins and Nucleic Acids, Cambridge University Press, Cambridge, 1987.
106 E. Fischer, Ber. Dtsch. Chem. Ges., 27 (1894) 2985.
107 G. Navon and G. Valensin, in H. Sigel (Ed.), Metal Ions in Biological Systems, Vol. 21, Dekker, Basle, 1987.
108 R.A. Dwek, Nuclear Magnetic Resonance in Biochemistry: Applications to Enzyme Systems, Oxford University Press, London, 1973.
109 I. Bertini and C. Luchinat, in I. Bertini, H.B. Gray, S.J. Lippard and J.S. Valentine (Eds.), Bioinorganic Chemistry, University Books, CA, 1992.

110 I. Bertini and C. Luchinat, in H. Sigel (Ed.), Metal Ions in Biological Systems, Vol. 15, Dekker, New York, 1983, p. 93.
111 L. Banci, I. Bertini, F. Briganti and C. Luchinat, New J. Chem., 15 (1991) 467.
112 P.A. Bottomly, in C.L. Partain et al. (Eds.), Nuclear Magnetic Resonance (NMR) Imaging, Vol. 2, Saunders, Philadelphia, 1988.
113 S.W. Young, B.B. Simpson, A.V. Ratner, C. Matkin and E.A. Carter, Magn. Reson. Med., 10 (1989) 1.
114 P. Niemi, H. Paajanen, H. Määttänen, K. Markku, M. Erkintalo, A. Alanen, P.B. Dean and M. Kormano, Magn. Reson. Med., 7 (1988) 311.
115 G. Navon, R. Panigel and G. Valensin, Magn. Reson. Med., 3 (1986) 876.
116 I. Bertini, F. Capozzi and C. Luchinat, Magn. Reson. Imaging, 9 (1991) 849.